MODELING THE ACOUSTIC BEHAVIOR OF A LIQUID ROCKET COMBUSTION CHAMBER WITH BAFFLES

Carlos d'andrade Souto, souto@iae.cta.br
Rogério Pirk, rogerio.pirk@iae.cta.br
General Comand of Aerospace Technology (CTA) – Institute of Aeronautics and Space (IAE) – Division of Integration and Tests (AIE) - Pça. Mal. Eduardo Gomes, 50 – Vila das Acácias – CEP:12231-970 – São José dos Campos – SP – Brasil

Abstract. Combustion instabilities occur when a great amount of energy is concentrated in one or more frequencies, generating pressure peaks much stronger than the background combustion noise. Liquid rocket engines can be affected by low and high frequency instabilities. The later is related to the interaction of chamber acoustics with combustion process or with propellant injection flow oscillations. Combustion instabilities had been present in the development of liquid rocket engines since the infancy of this technology in the World War II. It can affect the rocket's propulsion system performance even resulting in catastrophic failure and still remains a major design concern. High frequency acoustic instabilities can be treated by introducing in the combustion chamber passive acoustic devices like baffles and resonators. Baffles can slightly shift some specific acoustic frequencies but mainly introduce damping in the system response. Many researchers pointed out that, acoustic tests in combustion chambers can be performed under ambient conditions and cold - test results can be used to evaluate the chamber's eigenfrequencies during hot-firing tests. In this work the effect of placing some baffles into a combustion chamber is analyzed using the finite element method. The eigenfrequencies and the damping of some acoustic modes are calculated for the configurations with and without baffles.

Keywords: rockets, combustion instabilities, acoustics, finite elements

1. INTRODUCTION

Liquid rocket engines can be affected by combustion instabilities caused by the coupling of the chamber's acoustic modes with the combustion process. Baffles can be placed into the chamber in order to shift its acoustic eigenfrequencies and increase damping. The performance of such attenuation devices can be evaluated by cold tests and also by numerical modeling.

Acoustic instabilities occurs when the combustion couples with one or more chamber's acoustic modes, generating pressure oscillations that affect the engine's performance and safety operation. The pressure oscillations' amplitude can be reduced by changing the affected modes shifting its frequencies or introducing damping. Although the way that baffles attenuate pressure oscillations amplitude is not yet clearly understood (Laudien et al, 1996), the introduction of these kind of devices is a common strategy to reduce acoustic instabilities in liquid rocket combustion chambers (NASA, 1974).

For this application there are two kinds of baffles: circular and radial. The importance of some design parameters was shown by Natanzon (1986). The circular baffle radii, the total number of baffles of both types, its height and thickness are some parameters that must be object of careful analysis in order to obtain the best performance possible as a pressure oscillation attenuator, and also keeps baffle's structural integrity since it will be immersed in a high temperature environment and its cooling can became critical. This kind of analysis will not be object of this work.

In this work we analyze the effect of placing baffles in a combustion chamber. Frequency responses are numerically calculated using the finite element method for a chamber without and with baffles. In future works we intend to perform sensitivity analysis to check the baffle's design parameters influence and validate these numerical results with acoustic cold tests.

2. ACOUSTIC MODES AND COMBUSTION INSTABILITY

According to many authors like Laudien (1996) and Natanzon (1986) combustion instability in liquid rocket engines is mainly due to the tangential acoustic modes. The acoustic modes of a cylindrical cavity can be classified in: longitudinal, radial and tangential. In longitudinal modes pressure oscillations travels in the chamber symmetry axis and its nodal planes are parallel to the injector's face plate. In tangential modes the nodal planes contains the chamber symmetry axis and in radial modes there are cylindrical nodal surfaces co-axial with the chamber, as shown in Fig. 1.

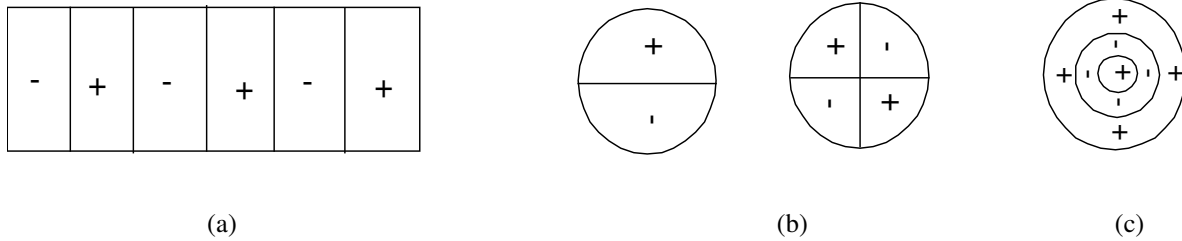(a)   (b)   (c)

Figure 1 –Acoustic modes of a cylinder: (a) longitudinal, (b) tangential e (c) radial

In Fig.1, a side view of a cylinder is shown in item (a) while itens (b) and (c) shown the top view of a cylinder. Since the combustion chambers are not perfect cylinders many modes are actually mixed ones.

3. ACOUSTIC MODELLING BY FINITE ELEMENTS

The Helmholtz equation witch governs the behavior of an acoustic cavity (Desmet, 2001) is:

$$\nabla^2 p - \frac{1}{c^2}\frac{\partial^2 p}{\partial^2 t} = Q \tag{1}$$

Where p is the acoustic pressure, c is the sound velocity, t is time and Q the acoustic source. The presence of rigid walls in the cavitiy's frontiers is considered by the natural boundary condition:

$$\frac{\partial p}{\partial n} = 0 \tag{2}$$

The problem can be discretized using the standard finite element method. Using the interpolation functions ($[N_f]$) one can write the pressures by (Zienkiewicz and Taylor, 1994):

$$p = [N_f]\{p_n\} \tag{3}$$

where $\{p_n\}$ is the nodal pressure vector.

A fluid domain at rest, considered inviscid, homogeneous, with no-rotational flow is governed by the Helmholtz equation. Assuming the conditions cited above and a fluid domain limited by rigid non absorbing walls, the Helmholtz equation can be discretized and the kinetic energy (T_f) and potential energy (U_f) could be write in the following form :

$$T_f = \tfrac{1}{2}\{p_n\}^T [H]\{p_n\} \tag{4}$$

$$U_f = \tfrac{1}{2c^2}\{\dot{p}_n\}^T [E]\{\dot{p}_n\} \tag{5}$$

Where $[E]$, $[H]$ are the compressibility and the volumetric matrices respectively and ρ_f is the fluid specific mass. Considering the free vibration's case for small oscillations and applying Lagrange's equations leads to:

$$[E]\{\ddot{p}_n\} + [H]\{p_n\} = \{q_n\} \tag{6}$$

Where $\{q_n\}$ is the acoustic sources nodal vector. Dissipative effects like acoustic damping or cavity walls with sound absorbing properties can be taking into account by including in the equation (6) the matrix [D]:

$$[E]\{\ddot{p}_n\}+[D]\{\dot{p}_n\}+[H]\{p_n\}=\{q_n\} \tag{7}$$

Considering the excitation and response harmonic,i.e.:

$$\{q_n\}=\{q\}e^{j\omega t} \tag{8}$$

$$\{p\}=\{p\}e^{j\omega t} \tag{9}$$

Putting equations (8) and (9) into equation (7), then:

$$\left(-\omega^2[E]+j\omega[D]+[H]\right)\{p\}=\{q\} \tag{10}$$

By solving equation (1) one can obtain the pressure nodal values in the frequency domain, $\{p(\omega)\}$.

4. ACOUSTIC CAVITY ANALYZED

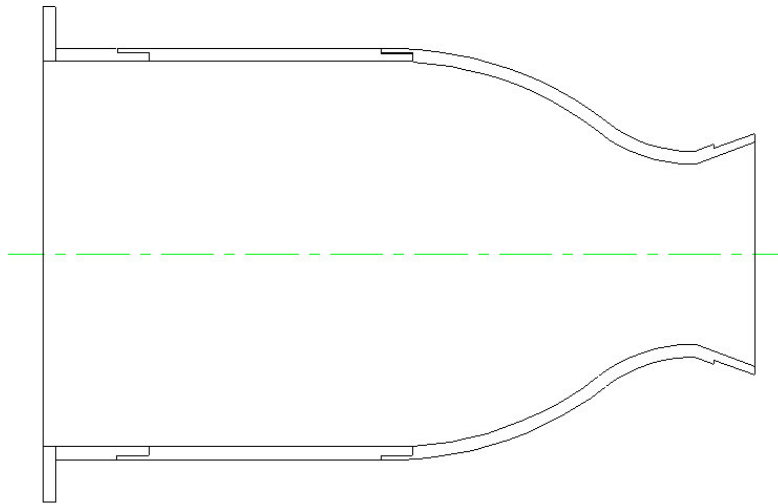The chamber's acoustic cavity is shown in Fig. 2.

Figure 2 – Combustion chamber analyzed

According to Laudien (1996) a (baffle height)/(chamber diameter) ratio of 0.1 and 5 radial baffles can introduce a high level of damping. A baffle system with these characteristics was placed on the injector's face plate shown in Fig. 3.
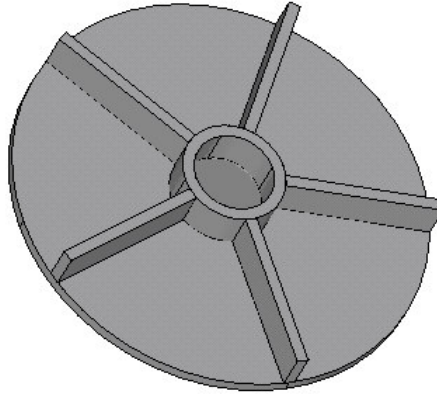
Figure 3: Baffles system analyzed

5. DAMPING CALCULATION

A finite element model of the acoustic cavity was created. The frequency response (pressure) to an acoustic excitation was calculated around the resonance peaks and the damping of each mode was so calculated by the half power bandwidth method. By this method the damping ratio of the r-mode is estimated by:

$$\eta_r = \frac{\omega_2 - \omega_1}{\omega_r} \qquad (11)$$

Where η_r is the damping ratio, ω_1 and ω_2 are frequencies close to the resonance peak corresponding to a 3 dB reduction of the amplitude in a logarithmic scale, as can be seen in Fig. 4.
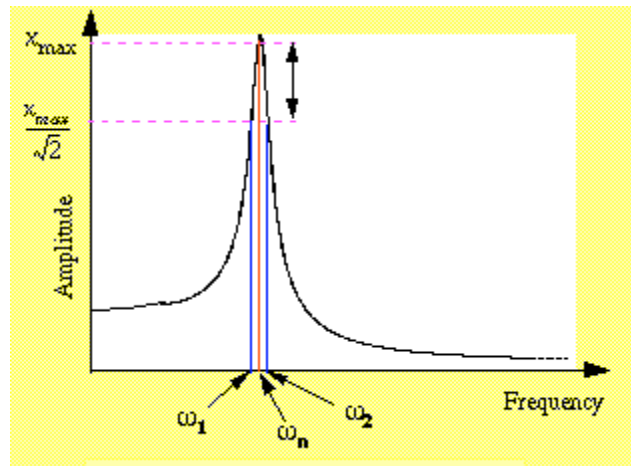

Figure 4 – Half power bandwidth method

6. FINITE ELEMENT MODEL

In Fig. 5 the acoustic mesh for the chamber cavity without baffles is displayed. The blue arrow shows the position of the acoustic excitation (prescribed unitary velocities). Figure 6 presents the mesh for the chamber with baffles. In both meshes 14,430 linear hexaedral elements with 15,281 nodes where used. A rigid wall boundary condition was applied to the part of the mesh corresponding to the throat. In a real chamber the flow in this region becomes supersonic and so the throat acts as rigid wall, reflecting the acoustic waves. In all others mesh frontiers an absorption coefficient of 0.005, the same value used by Sohn, et al (2007), in an experiment with a similar chamber.
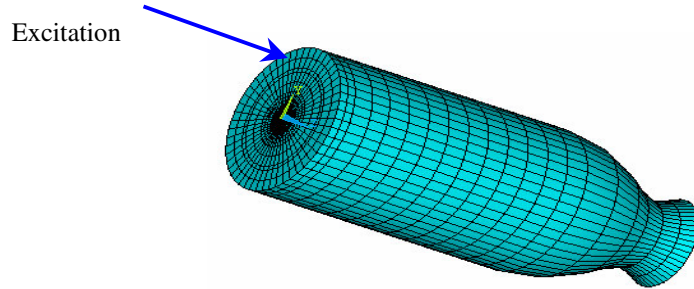
Excitation

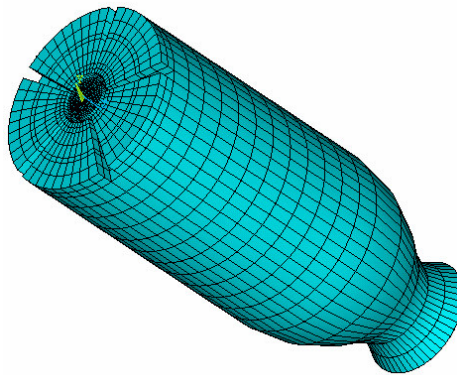Figure 5: Mesh of the combustion chamber without baffles

Figure 6: Mesh of the combustion chamber without baffles

7. RESULTS

The responses were calculated in three internal nodes. These nodes coordinates are displayed in Tab. 1 and the coordinate system used is displayed in Fig. 8.
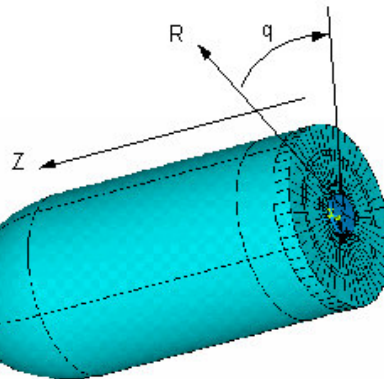

Figure 7 – Coordinate system

Table 1 – Coordinates of the points where the response were calculated

Point	R	q	Z
1	8 mm	-72 °	39 mm
2	65 mm	0 °	18 mm
3	60 mm	28,80 °	60 mm

The frequency responses calculated in the points 1, 2 and 3 for the first 5 tangential modes are shown in Figs 8 to 14. Those curves were used to evaluate damping using equation. (11)

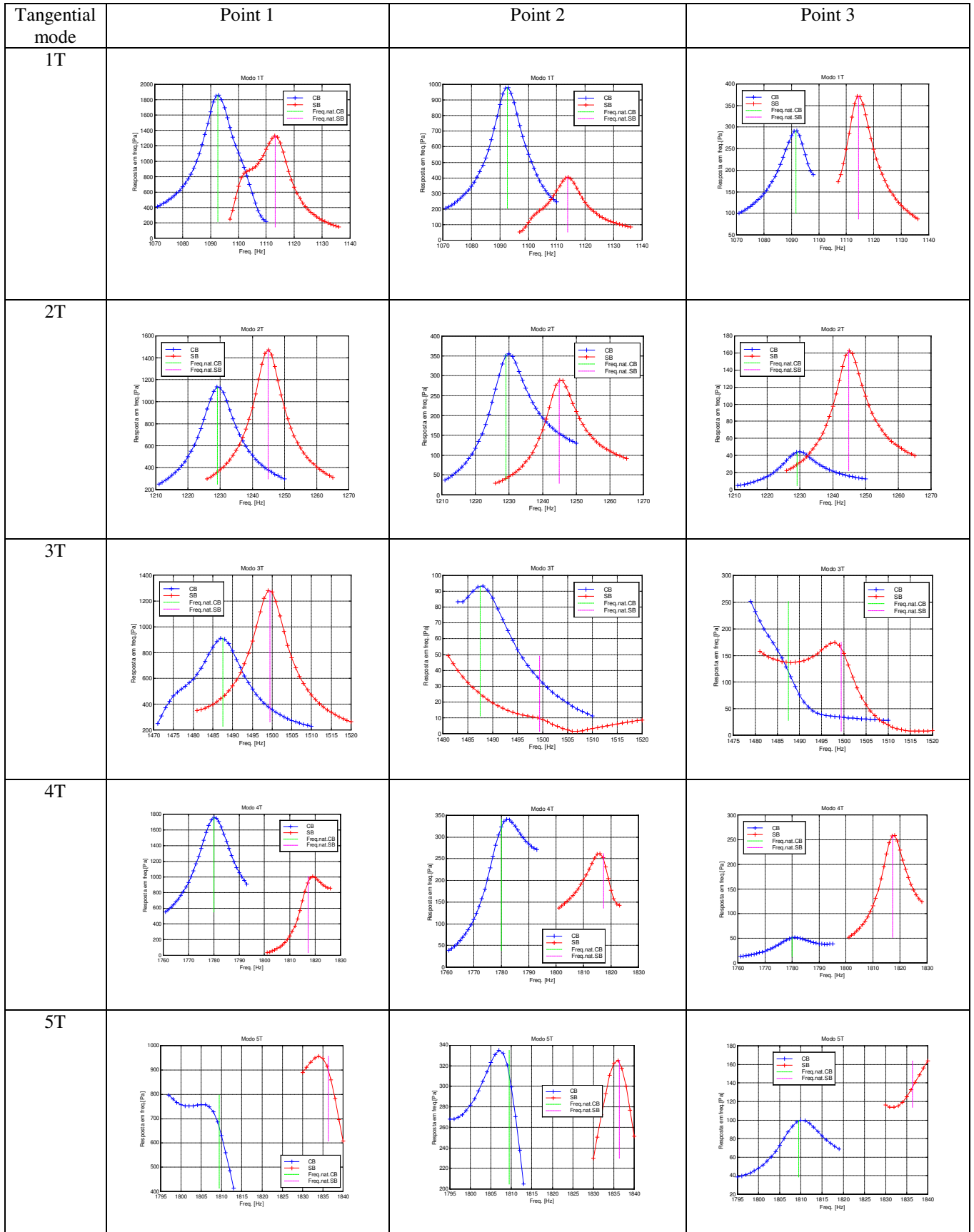| Tangential mode	Point 1	Point 2	Point 3
1T			
2T			
3T			
4T			
5T			

Figure 8: Frequency responses for the chamber without (SB in red) and with baffles (CB in blue)

Tables. 2 and 3 describe the calculated natural frequencies and dampings for the meshes with and without baffles, respectively.

Table 2 – Natural frequencies and dampings for the mesh with baffles

Mode	Frequencies [Hz]	Damping in point 1	Damping in point 2	Damping in point 3
1T	1092.46	0.009738	0.008861	0.008846
2T	1229.18	0.008389	0.009621	0.007193
3T	1487.50	0.008114	0.007010	Too high
4T	1780. 10	0.007284	0.006493	0.007033
5T	1809.42	0.015542	0.005417	0.008932

Table 3 – Natural frequencies and dampings for the mesh without baffles

Mode	Frequencies [Hz]	Damping in point 1	Damping in point 2	Damping in point 3
1T	1113.88	0.012194	0.008635	0.008875
2T	1244.86	0.006680	0.007893	0.006278
3T	1499.39	0.005583	Too high	0.004802
4T	1817.17	0.004269	0.007927	0.005289
5T	1836.40	0.005705	0.006281	0.007440

Table 4 shows the increasing (positive) or decreasing (negative) in damping for the calculated frequency responses for the points 1, 2 and 3.

As can be seen in Fig. 8, the third tangential mode shows high damping in both configurations (with and without baffles) respectively in points 3 and 2 and for this reason it was not calculated.

Table 4 – Changing in damping due to the introduction of baffles

Mode	Changing in the damping point 1 (%)	Changing in the damping point 2 (%)	Changing in the damping point 3 (%)
1T	-20.14	2.61	-0.32
2T	25.59	21.90	14.59
3T	45.34	-	-
4T	70.62	-18.09	32.98
5T	172.43	-13.76	20.05

On the contrary of was expected, the results for the first tangential mode (presented in Tab. 4) did not increase significantly. Usually the introduction of baffles affects more strongly the first tangential mode reducing its damping (Laudien et al 1996). In this specific case, for the mesh without baffles, the 3L (third longitudinal) and the 1T (first tangential) modes are too close in frequency. The third longitudinal mode interferes in the first tangential mode, making its resonance peak more damped. When the baffles are introduced these modes become less closer in frequency and so its proximity does not increase the damping anymore and the damping is reduced.

The value adopted for the walls' absorption coefficient can increase the damping of all modes. For the 1T mode, its proximity to the 3L mode combined with a "strong " damping due to absorption may produce a particularly damped peak. To evaluate the influence of the walls' absorption coefficient on damping of the 1T mode we calculated the response frequency for walls' absorption coefficient values of 0; 0.001 and 0.002. Table 5 shows the shifts in damping after the introduction of baffles for the new values of walls' absorption coefficient.

Table 5 – Changing in the damping for mode 1T (%) x chamber wall
absorption coefficient after the introduction of baffles

Absorption coefficient	Changing in the damping point 1 (%)	Changing in the damping point 2 (%)	Changing in the damping point 3 (%)
0	36.5983	36.5983	36.0373
0.001	8.69049	10.8984	15.1464
0.002	1.78677	5.27355	15.1656
0.005	-20.1393	2.61104	-0.322844

7.CONCLUSIONS

Due to the introduction of baffles the longitudinal modes' frequencies were increased and the tangential modes frequencies were decreased. The damping was augmented for some modes and reduced for others. It can be seen in the response calculated in the point 1 for the 1T mode of the unbaffled chamber (Fig. 8) that the 3L mode peak is mixed with 1T mode peak, making its damping bigger. In the response calculated in points 2 and 3 the damping was very slightly affected, as can be seen in Tab. 4.

The results displayed in Tab.5 shows that the walls' absorption coefficient can play an important role in the baffles' efficiency of introducing damping. The smaller the walls' absorption coefficient, the bigger the damping introduced by the baffles. Also, when the walls' absorption coefficient is reduced, the agreement among the damping calculated by the responses in all the 3 points became higher.

The first tangential mode is usually considered the most important for acoustic instabilities and so the one where damping must be introduced (Sohn et al, 2007) and (Huzel, 1992). However, only hot tests can show which frequencies are really affected by acoustic instabilities.

The future steps of this work can include a sensitivity analysis of some baffle design parameters like its height, quantity as well as the experimental validation of this results in cold tests, with the evaluation of chamber's walls' absorption coefficient.

8.ACKNOWLEDGEMENTS

9. REFERENCES

Desmet, W., Vanderpite, D., 2001 Course notes *Finite element method in acoustics*, Leuven

Huzel, D.K., Huang, D. H., 1992 "*Modern Engineering for Design of Liquid-Propellant Rocket Engines",* vol.147 Progress in Astronautics and Aeronautics, AIAA, Washington.

Laudien, E. et al., 1996 *Experimental Procedures Aiding the Design of Acoustic Cavities*, DASA- Deutsche Aerospace AG, Liquid Rocket Engine Combustion Instability, Progress in Astronautics and Aeronautics, Chapter 14, volume 169.

NASA SP 8113 "*Liquid Rocket Engine Combustion Stabilization Devices*" , Novembro de 1974

Natanzon, M. S., 1986 "*Combustion Instability*" , Mashinostroyenie, Moscow. Tradução em inglês

Sohn, C., Park, I., Kim, S. Kim, H. J., 2007 "*Acoustic tuning of gas liquid scheme injectors for acoustic damping in a combustion chamber of a liquid rocket engine"*, Journal of Sound and Vibration 304, pp.793-810, 2007

Zienkiewicz, O.C., Taylor, R. L.,1994 "*The Finite Element Method*" 4th edition Mc Graw Hill

10. RESPONSIBILITY NOTICE

The authors are the only responsible for the printed material included in this paper.